MOLECULAR AND CELLULAR BIOLOGY, Nov. 2011, p. 4550–4562 Vol. 31, No. 22
0270-7306/11/$12.00 doi:10.1128/MCB.05817-11

SCIMP, a Transmembrane Adaptor Protein Involved in Major Histocompatibility Complex Class II Signaling▽†

Peter Draber,[1] Ivana Vonkova,[1] Ondrej Stepanek,[1] Matous Hrdinka,[1] Marketa Kucova,[1] Tereza Skopcova,[1] Pavel Otahal,[1] Pavla Angelisova,[1] Vaclav Horejsi,[1] Mandy Yeung,[2] Arthur Weiss,[2] and Tomas Brdicka[1]*

Institute of Molecular Genetics, Academy of Sciences of the Czech Republic, Prague 14220, Czech Republic,[1] and Howard Hughes Medical Institute and Department of Medicine, University of California, San Francisco, San Francisco, California 94143-0795[2]

Received 15 June 2011/Returned for modification 14 July 2011/Accepted 2 September 2011

Formation of the immunological synapse between an antigen-presenting cell (APC) and a T cell leads to signal generation in both cells involved. In T cells, the lipid raft-associated transmembrane adaptor protein LAT plays a central role. Its phosphorylation is a crucial step in signal propagation, including the calcium response and mitogen-activated protein kinase activation, and largely depends on its association with the SLP76 adaptor protein. Here we report the discovery of a new palmitoylated transmembrane adaptor protein, termed SCIMP. SCIMP is expressed in B cells and other professional APCs and is localized in the immunological synapse due to its association with tetraspanin-enriched microdomains. In B cells, it is constitutively associated with Lyn kinase and becomes tyrosine phosphorylated after major histocompatibility complex type II (MHC-II) stimulation. When phosphorylated, SCIMP binds to the SLP65 adaptor protein and also to the inhibitory kinase Csk. While the association with SLP65 initiates the downstream signaling cascades, Csk binding functions as a negative regulatory loop. The results suggest that SCIMP is involved in signal transduction after MHC-II stimulation and therefore serves as a regulator of antigen presentation and other APC functions.

The adaptive immune response is initiated by T cell recognition of antigen peptide-loaded major histocompatibility complex (MHC) glycoproteins present on the surfaces of professional antigen-presenting cells (APCs), such as dendritic cells (DCs), macrophages, and B cells (41, 45). This leads to the formation of the immunological synapse (IS) at the cell-cell contact site. The hallmark of the IS is accumulation of T cell receptors (TCRs) paired with peptide-MHC, together with pairs of adhesion and costimulatory molecules (14).

Numerous proteins participating in the formation of IS have been described as constituents of plasma membrane microdomains, such as lipid rafts or tetraspanin-enriched microdomains (TEMs). Lipid rafts are lipid-based structures enriched with cholesterol, sphingolipids, and glycosphingolipids that contain certain glycosylphosphatidylinositol (GPI)-linked, transmembrane or acylated cytoplasmic proteins (33). In contrast, TEMs are based on protein-protein interactions among different tetraspanins, such as CD9, CD37, CD53, CD81, or CD82. All tetraspanins share a similar structure, including four transmembrane domains and structurally conserved small and large extracellular domains. Tetraspanins can also interact with additional transmembrane proteins, including integrins and MHC-II, leading to the formation of membrane platforms (23, 49).

Active signal transduction takes place on both sides of the IS. This leads to cross talk between APCs and T cells, required for efficient antigen presentation. In addition, formation of IS in DCs results in apoptosis inhibition and prolonged life span (40). Antigen presentation inducing activation of naive T cells is a primary function of DCs. Although B cells too are able to activate T lymphocytes, the primary function of antigen presentation in B cells appears to be the soliciting of T cell help required for productive activation (11). An important role is played by costimulatory molecules, such as CD40, but many of the signaling events occurring at the B cell side of IS are also dependent on the presence of specific peptide–MHC-II complexes and thus presumably on direct engagement of MHC-II molecules. However, the complexity of IS, as well as the ability of MHC-II to transmit signals in both directions, makes the analysis of direct involvement of MHC-II in APC signal transduction relatively difficult. One possibility to overcome this problem is antibody-mediated cross-linking of MHC-II molecules. Interestingly, this can recapitulate a number of events observed during B cell interaction with T cells, including cytoskeleton reorganization, an increase in tyrosine phosphorylation and the calcium concentration, proliferation, differentiation, or apoptosis (1). In addition, high sensitivity of certain B cell lymphomas to cell death following MHC-II cross-linking make anti-MHC-II antibodies potential therapeutic agents (9, 37).

The mechanism by which the signaling is initiated upon MHC-II stimulation is still incompletely defined. In B cells, MHC-II-associated molecules, such as signal-transducing sub-

* Corresponding author. Mailing address: Institute of Molecular Genetics, ASCR, Videnska 1083, 142 20 Prague, Czech Republic. Phone: (420)241062467. Fax: (420)244472282. E-mail: tomas.brdicka@img.cas.cz.

† Supplemental material for this article may be found at http://mcb.asm.org/.

▽ Published ahead of print on 19 September 2011.

units of B cell receptor (BCR) Igα/Igβ (31), CD19 (5), or the innate immune signaling adaptor MPYS/STING (26), are thought to mediate signal transmission. Partitioning to lipid rafts (2) or tetraspanin-enriched microdomains (30) may also equip MHC-II molecules with signaling capabilities. As a result, MHC-II signaling in B cells is rather complex and involves BCR signaling machinery, as well as other BCR-independent mechanisms. However, there still are large gaps in our understanding of precise pathways and molecules involved.

In contrast, signal propagation on the T cell side of IS is well defined. TCR engagement in the IS leads to subsequent activation of Src and Syk family kinases and tyrosine phosphorylation of a number of molecules, including the transmembrane adaptor protein (TRAP) LAT. LAT is a critical component of several signaling pathways, mainly due to its ability to recruit a complex of phospholipase C gamma 1 (PLC-γ1) with the adaptors Gads and SLP76 (16).

SLP76 and its related homologue SLP65 (also known as BLNK or BASH) are involved in the transduction of signals emanating from various immunoreceptors, like the TCRs, BCRs, or Fc receptors (28). Following cell activation, these adaptors are brought to the plasma membrane. Their recruitment is largely dependent upon tyrosine phosphorylation of transmembrane proteins and can be accomplished either indirectly, as in the case of the inducible association between LAT and SLP76 mediated via a cytosolic adaptor, Gads, or directly, as in the complex of SLP65 and the BCR subunit Igα (13). Once localized at the membrane, the SLP65/SLP76 proteins become phosphorylated by Syk family kinases and form complexes with various effector molecules, such as Nck and Vav, Tec family kinases, and PLC-γ1 or PLC-γ2. This leads to initiation of downstream responses, including actin cytoskeleton remodeling, calcium flux, and activation of mitogen-activated protein kinases (MAPKs).

Reversible membrane localization is a key feature of another critical regulatory circuit of immunoreceptor signaling, involving the cytoplasmic inhibitory kinase Csk. Csk inhibits Src family kinases by phosphorylating the inhibitory tyrosine near their C termini, an event necessary for setting a proper threshold for numerous signaling pathways (10). In order to reach its substrates, Csk must be recruited to the plasma membrane. This process is in part mediated by the lipid raft-associated TRAPs PAG (6, 27) and LIME (7, 22).

In this study, we describe the discovery of a new TRAP which binds both the Src homology 2 (SH2) domain of the inhibitory kinase Csk and the SH2 domains of the SLP65 and SLP76 adaptors. Based on the described observations and the fact that this protein has to fulfill its function with only a comparably small number of 145 amino acids (aa) constituting its sequence, we decided to call it *S*LP65/SLP76, *C*sk-*i*nteracting *m*embrane *p*rotein (SCIMP). We provide an initial characterization of SCIMP, which reveals expression restricted to APCs, association with TEMs, localization in the IS, and involvement in signaling downstream of MHC-II molecules.

MATERIALS AND METHODS

SCIMP identification. The ScanProsite tool at the ExPASy Proteomics server (http://www.expasy.org/tools/scanprosite/) (12) was employed to generate the list of proteins containing the consensus Csk SH2 domain binding motif: Y-[A/S/T]-X-[V/P]-[N/Q/C]-[K/R] (7). The resulting list was submitted to the TMHMM server (http://www.cbs.dtu.dk/services/TMHMM-2.0/) (29, 46) to detect putative transmembrane domains. This step was then followed by manual selection of potentially interesting proteins.

Antibodies. Antibodies to the following antigens were used in this study: Myc (9B11), PLC-γ1, PLC-γ2, phosphorylated PLC-γ1 (P-PLC-γ1) (Y783), P-PLC-γ2 (Y1217), phosphorylated extracellular signal-regulated kinase 1 and 2 (P-Erk1/2) (T202/Y204), P-MEK1/2 (S217/221), and phosphorylated p90 ribosomal S6 kinase (P-p90RSK) (S380) were from Cell Signaling Technology; Erk2, Lyn, SLP65 (2B11), Grb2 (C-23), and Csk were from Santa Cruz Biotechnology; CD81 (M38) was from Exbio; P-Tyr (4G10) was from Upstate Biotechnology; Fc Block (2.4G2) was from BD Biosciences; mouse MHC-II I-A/I-E-biotin (M5/114.15.2) was from BioLegend; goat anti-mouse antibody–fluorescein isothiocyanate (FITC) and Thy1.1-FITC (HIS51) were from eBioscience; mouse Igμ, human Igμ, and horseradish peroxidase (HRP)-conjugated goat anti-mouse light-chain-specific antibodies were from Jackson ImmunoResearch; glyceraldehyde-3-phosphate dehydrogenase (GAPDH), HRP–goat anti-mouse specific IgG, HRP–rabbit anti-goat antibody, and HRP–rabbit anti-chicken antibody were from Sigma-Aldrich; HRP–goat anti-rabbit antibody was from Bio-Rad; goat anti-mouse antibody–Alexa Fluor 488 and goat anti-mouse antibody–Alexa Fluor 568 were from Molecular Probes; CD19 (B-d3) was kindly provided by J. Wijdenes (Innotherapie, Besançon, France); CD37 (HD28) was kindly provided by G. Moldenhauer (DKFZ, Heidelberg, Germany); CD3ε (MEM-57), CD56 (MEM-188), CD14 (MEM-18), CD25 (MEM-145), MHC-II (SLE-01), NTAL (NAP-04), PAG (MEM-255), CD53 (MEM-53), CD8 (control for mouse IgG1, MEM-146; control for mouse IgG2a, MEM-31), CD45 (MEM-28), and SLP76 (SLP76/3) were prepared at Laboratory of Molecular Immunology, IMG ASCR (Prague, Czech Republic).

Rabbit polyclonal antibodies against human and murine SCIMP were prepared by immunization of rabbits with recombinant proteins corresponding to intracellular parts of human SCIMP (aa 43 to 145) or murine SCIMP (aa 32 to 150) produced in *Escherichia coli*. Mouse monoclonal antibodies to human SCIMP were generated by standard techniques using splenocytes of mice (F1 hybrids of BALB/c × B10) immunized with the human recombinant protein described above and Sp2/0 myeloma cells as a fusion partner.

Cell lines and primary cells. All cell lines were cultured at 37°C with 5% CO_2 in the following media, supplemented with 10% fetal calf serum and antibiotics: Ramos, Raji, Daudi, and THP1 cell lines (all from ATCC) in RPMI 1640, HEK293FT cells (Invitrogen) and Phoenix Ampho cells (Origene) in Dulbecco's modified Eagle medium (DMEM), and K46 cells (kindly provided by J. Cambier, National Jewish Medical Research Center, Denver, CO) in Iscove's modified Dulbecco's medium (IMDM).

Human peripheral blood lymphocytes (PBLs) were prepared from buffy coats obtained at Thomayer University Hospital (Prague, Czech Republic) using Ficoll-Paque Plus (GE Healthcare) gradient centrifugation (900 × *g* for 30 min). To isolate different PBL subpopulations, T cells, B cells, NK cells, and monocytes were labeled with CD3, CD19, CD56, or CD14 antibodies, respectively, followed by FITC-conjugated secondary antibodies and anti-FITC magnetic beads (Miltenyi Biotec), and separated by positive selection on an AutoMACS magnetic cell sorter (Miltenyi Biotec). Purity was confirmed by fluorescence-activated cell sorter (FACS) analysis. Human Peripheral blood monocyte-derived dendritic cells (MDDCs) were obtained by differentiation of monocytes in complete RPMI 1640 medium containing interleukin 4 (IL-4) (10 ng/ml; PeproTech) and granulocyte-macrophage colony-stimulating factor (GM-CSF) (100 ng/ml, Leucomax; Novartis) for 8 days. For isolation of granulocytes, a gradient composed of Histopaque 1119 (Sigma-Aldrich), overlaid by Ficoll-Paque Plus and freshly collected blood from healthy donors, diluted with phosphate-buffered saline (PBS), was prepared and centrifuged (900 × *g* for 30 min). Granulocytes were collected from the interface between Ficoll-Paque and Histopaque 1119 layers. In addition, erythrocytes were isolated from the pellet and subjected to hypotonic lysis in 0.04% acetic acid to obtain red blood cell membranes (RBC ghosts). Platelets were prepared from the top phase of the gradient by two-step centrifugation (400 × *g* for 10 min to remove cells and large particles and 600 × *g* for 10 min to pellet platelets).

Mouse organs were isolated from C57BL/6 mice (Animal Facility of IMG ASCR, Prague, Czech Republic) sacrificed by cervical dislocation. Splenic B cells were prepared by negative selection using CD43 and CD11b magnetic beads (Miltenyi Biotec).

For SCIMP expression analysis, murine organs and tissues were snap-frozen in liquid nitrogen, homogenized in grinding mortar, and lysed in 2% SDS. As an exception, splenocytes and PBLs were first incubated with ACK buffer (ISS mM NH_4Cl, 10 mM $KHCO_3$, 0.1 mM EDTA [disodium salt]) to remove red blood cells and then directly lysed in 2% SDS. Bone marrow cells isolated from femurs and human blood cells were directly lysed in 2% SDS. All samples were centri-

fuged (70,000 × *g* for 30 min) to remove nuclei and debris. Protein concentrations were measured as absorbance at 280 nm and adjusted to obtain equal protein concentrations in all samples.

Where applicable, the procedures were performed after obtaining an informed consent from the donors and in accordance with national ethical guidelines. They were also approved by the Animal Care and Use Committee of the Institute of Molecular Genetics (Academy of Sciences of the Czech Republic).

RNA and RT-qPCR. A human normal tissue FirstChoice RNA survey panel and lymph node FirstChoice RNA were purchased from Ambion. Total RNA (1 μg) was transcribed using SuperScript III reverse transcriptase (RT) (Invitrogen) or RevertAid reverse transcriptase (Fermentas) with a combination of random pentadecamer and anchored oligo(dT)$_{20}$ primers. RT-quantitative PCR (qPCR) was carried out using LightCycler 480 SYBR green I master chemistry (Roche). Primers specific for human SCIMP cDNA were as follows: fwd-1, 5′-AGTCGC CAGTTCAATTACCG-3′; rev-1, 5′-GACTTGGGGCTTCCTGTG-3′, and fwd-2, 5′-TGCTCACATATGGATACTTTCACA-3′; rev-2, 5′-GGCCACAGCT AAGATGATCC-3′. RT-qPCR data (C_T values) were normalized to reference gene GAPDH data and analyzed using the GenEx software program (MultiD).

DNA constructs, cloning, and cell transfections. Human SCIMP cDNA was cloned from a leukocyte cDNA library (Clontech Laboratories) using the primers 5′-caGGATCCgctcacatatggatactttcacag and 5′-gtGAATTCtcaaaatgatgctttttcag tatt (restriction sites are in capital letters) and ligated into BamHI/EcoRI sites of pcDNA3. Mouse SCIMP was cloned from mouse splenic cDNA using the primers: 5′-gtGAATTCtcccacagcaatgagttggtg and 5′-gtCTCGAGctaaaacgagctgtgtaa acccacttc and ligated into EcoRI/XhoI sites of pcDNA3.

For immunoprecipitation experiments, the Myc coding sequence was added after the last codon of human SCIMP and this construct was cloned into MSCV-IThy1.1 (a retroviral vector with internal ribosome entry site (IRES)-Thy1.1 sequence for simultaneous expression of the Thy1.1 surface reporter; kindly provided by P. Marrack, National Jewish Health, Denver, CO). Y69F, Y107F, Y124F, and Y131F tyrosine mutants were prepared using PCR mutagenesis. The proline-rich sequence deletion mutant lacking aa 81 to 104 was prepared by fusion PCR. To obtain SCIMP-green fluorescent protein (GFP), SCIMP was cloned into pEGFP-N3 (Clontech Laboratories), and SCIMP-GFP sequence was subsequently ligated into MSCV-IThy1.1. CD25-SCIMP chimeras were prepared by cloning the sequence of extracellular part of human CD25 (coding aa 1 to 240), followed by sequence of SCIMP (coding aa 13 to 145, with or without a C-terminal Myc tag) into MSCV-IThy1.1. All constructs were sequenced.

The following constructs were used for cotransfection experiments in HEK293: Lyn in pcDNA3 (kindly provided by S. Watson, University of Birmingham, Birmingham, United Kingdom), c-Src in pSM (kindly provided by D. Littman, New York University School of Medicine), FynT in pEF-BOS (kindly provided by B. Schraven, Otto-von-Guericke University, Magdeburg, Germany), and Syk in pRK5 (kindly provided by W. Kolanus, University of Cologne, Cologne, Germany).

The Lipofectamine 2000 reagent (Invitrogen) was used according to the manufacturer's instructions for transfection of both HEK293FT (cotransfection studies) and Phoenix Ampho cells (production of viral particles using the MSCV-IThy1.1 vector). Retrovirus-containing supernatants were supplemented with Polybrene (10 μg/ml; Sigma-Aldrich) and added to cells. Cells were then centrifuged at 1,250 × *g* for 90 min. Infected cells were labeled with anti-Thy1.1-FITC antibody followed by anti-FITC magnetic beads and isolated on an AutoMACS cell sorter.

Cell activation. Cells (5×10^7 cells/ml) were stimulated with 1 mM pervanadate for 20 min or with the required antibody (10 μg/ml) for 2 min or as indicated in serum-free medium at 37°C. In the case of MHC-II cross-linking, Fc receptors were blocked by incubation with 2.4G2 antibody on ice. Primary biotinylated antibody (10 μg/ml) was then added for 30 min, cells were washed and resuspended in warm medium, and streptavidin (10 μg/ml; Jackson ImmunoResearch) was added after 5 min. Cells were incubated at 37°C as appropriate. Samples were solubilized in lysis buffer (for immunoprecipitation studies, see below) or in SDS-PAGE sample buffer (for analysis of signaling pathways by phospho-specific antibodies).

Biochemical procedures. Lysis with detergents was carried out by solubilization of 5×10^7 cells in 1 ml of cold lysis buffer (20 mM Tris [pH 7.5], 100 mM NaCl, 1 mM Pefabloc [Sigma-Aldrich], 5 mM iodoacetamide, 50 mM NaF, 1 mM Na_3VO_4, 10 mM EDTA, 10% [vol/vol] glycerol) supplemented with 1% (wt/vol) detergent {laurylmaltoside, Brij 98, NP-40, or 3-[(3-cholamidopropyl)-dimethylammonio]-1-propanesulfonate [CHAPS], as required} for 30 min. Nuclei and debris were removed by centrifugation (16,000 × *g* for 10 min).

For immunoprecipitation, detergent lysates were incubated for 1 h with primary antibody (500× diluted), followed by 2 h of incubation with protein A/G Plus-agarose beads (Santa Cruz Biotechnology). When preclearing was used, this procedure was performed first with the control and then repeated with specific antibodies. After washing, immunoprecipitates were eluted with 60 μl SDS-PAGE sample buffer.

For flotation in sucrose density gradient, 0.5-ml aliquots of cell lysates (without glycerol) were mixed with 0.5 ml 80% (wt/vol) sucrose in lysis buffer in an ultracentrifuge tube and overlaid with 3.5 ml 35% sucrose and finally 0.5 ml of lysis buffer. Samples were subjected to ultracentrifugation (20,000 × *g* for 20 h), and 0.6-ml fractions were collected from the top of the gradient.

For gel filtration, 0.2-ml aliquots of detergent lysate were separated on a column containing 2 ml of Sepharose 4B and continually washed with lysis buffer with the corresponding detergent, and 0.2-ml fractions were collected.

For cell fractionation, 9×10^7 cells were resuspended in 0.5 ml of cold hypotonic buffer (10 mM HEPES [pH 7.4], 42 mM KCl, 5 mM $MgCl_2$, 1 mM Pefabloc, 5 mM iodoacetamide, 50 mM NaF, 1 mM Na_3VO_4, 10 mM EDTA) and mechanically disintegrated by forcing the cell suspension 10 times through a 25-gauge injection needle. The homogenate was centrifuged at 400 × *g* for 10 min to pellet the nuclear fraction, followed by centrifugation at 25,000 × *g* for 10 min to pellet the membrane fraction. The resulting supernatant contained the cytoplasmic fraction.

An acyl-biotinyl exchange reaction was carried out as previously described (48). Isolated plasma membrane fraction proteins from 5×10^7 cells were incubated with *N*-ethylmaleimide to block free thiols. The samples were then incubated with hydroxylamine to remove palmitate residues (this step was omitted with control samples), and the resulting free thiol groups were labeled with biotin-HPDP (Pierce, Thermo Fisher Scientific). Biotinylated proteins were immunoprecipitated on streptavidin-agarose beads and eluted with SDS-PAGE sample buffer.

Calcium flux measurement. Cells were loaded with 2 μg/ml calcium indicator dye Fluo-4 (Invitrogen). Samples were analyzed by using a FACSCalibur flow cytometer for 30 s at rest and then another 3 min after activation with CD25 antibody (10 μg/ml). The calcium response index was calculated as the percentage of cells with Fluo-4 fluorescence higher than the 95th percentile of resting cells during the time interval between 10 and 20 s. Data were analyzed using the FlowJo software program (TreeStar).

Microscopy. For live cell microscopy, Ramos or Daudi B cells expressing SCIMP-GFP were loaded with staphylococcal enterotoxin E (SEE) (1 μg/ml; Toxin Technology) and transferred into Lab-Tek chambered cover glass (Nunc; Thermo Fisher Scientific), and DDAO (Molecular Probes, Invitrogen)-labeled Jurkat T cells were subsequently added at a ratio of 1:1. Cells were observed in a climate chamber (37°C, 5% CO_2) under a Leica DMI6000 B fluorescence microscope using a 40× objective lens (Leica Microsystems), and images were acquired every 30 s. Eventually, the percentage of conjugates with SCIMP-GFP localized at the IS was assessed after 1 h.

For antibody staining, the spontaneously polarized Ramos cells or SEE-induced conjugates were fixed with 4% (wt/vol) paraformaldehyde, permeabilized with 0.1% (wt/vol) Triton X-100, and blocked in PBS with 0.5% bovine serum albumin (BSA), 5% human AB serum, and 5% goat serum. After staining with primary and Alexa Fluor 568-conjugated secondary antibodies, the samples were mounted in Mowiol medium and observed with a Leica TCS SP5 confocal microscope using a 63× objective lens (Leica Microsystems). Data were analyzed using the LAS AF software program (Leica Microsystems).

Lentiviral shRNA-mediated knockdown. The vector pLKO.1, containing small-hairpin RNA (shRNA) sequences against SCIMP (shRNA 1, TRCN0000267281; shRNA 2, TRCN0000267278; shRNA 3, TRCN0000283513), and empty vector were purchased from Sigma, mixed with ViraPower packaging mix (Invitrogen) according to the manufacturer's instructions, and transfected to HEK293FT using the Lipofectamine 2000 reagent. Virus-containing supernatants were concentrated with PEG-it virus precipitation solution (System Biosciences) supplemented with Polybrene (10 μg/ml) and added to the K46 cell line. Cells were cultured in the presence of puromycin (6 μg/ml; InvivoGen). Stable clones obtained were analyzed for expression of SCIMP. For immunoblot analysis of signaling defects, the Odyssey infrared imaging system (LI-COR Biotechnology) was used.

RESULTS

SCIMP identification and primary structure. To identify new candidate proteins that could recruit Csk to the proximity of its substrates at the plasma membrane, we searched the Uniprot protein database for transmembrane proteins that could potentially interact with the Csk SH2 domain. In addition to the well-

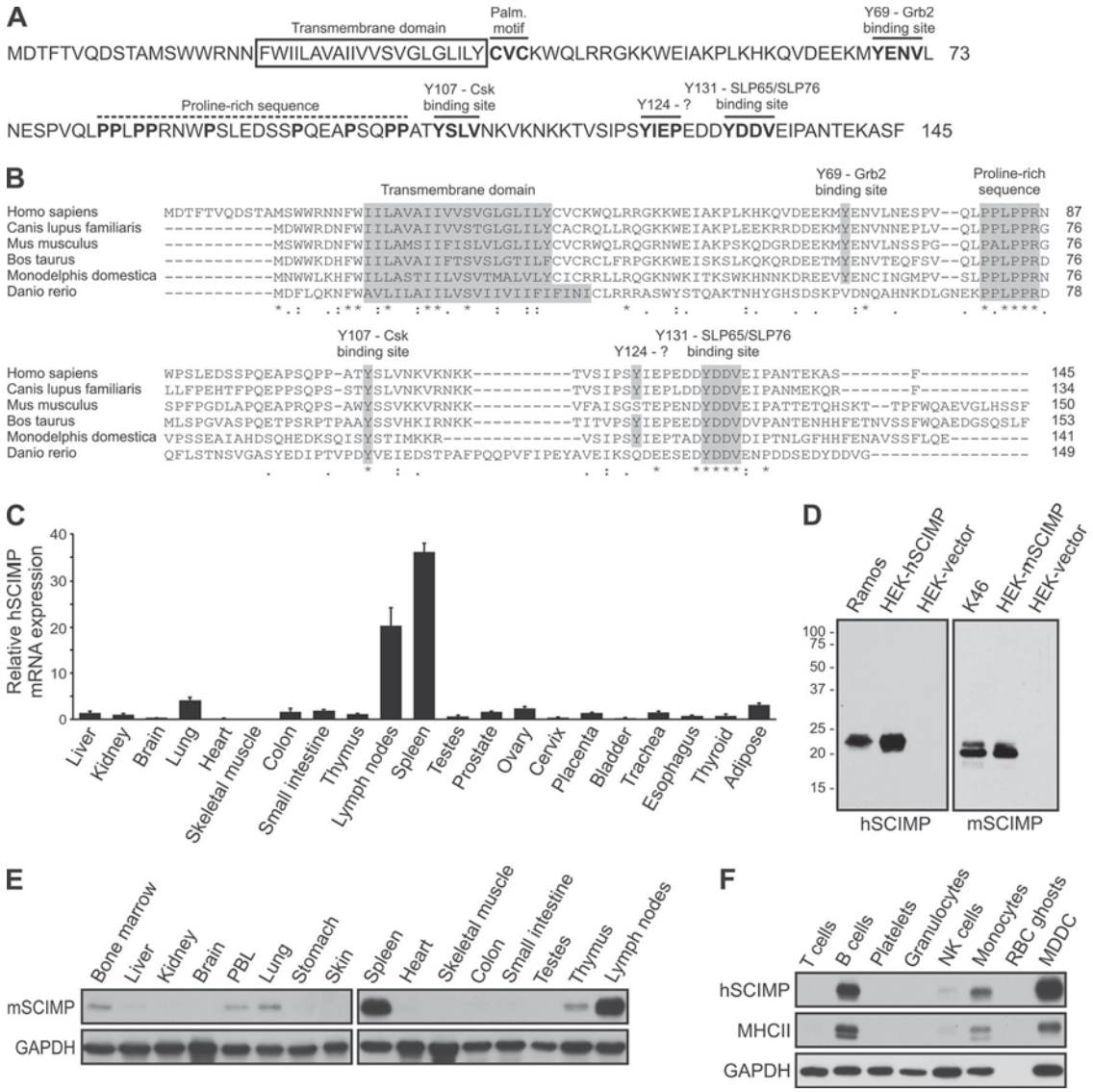

FIG. 1. SCIMP is a transmembrane adaptor protein expressed in antigen-presenting cells. (A) Sequence of human SCIMP. Positions of the transmembrane domain, palmitoylation motif, proline-rich sequence, and predicted Grb2, Csk, and SLP65/SLP76 binding sites are indicated. (B) Comparison of SCIMP sequences from human (*Homo sapiens*), dog (*Canis lupus familiaris*), mouse (*Mus musculus*), cattle (*Bos taurus*), opossum (*Monodelphis domestica*), and zebrafish (*Danio rerio*). The transmembrane domain, highly conserved part of the proline-rich sequence and SLP65/SLP76 binding motif, as well as other conserved tyrosine residues, are highlighted, and positions of corresponding tyrosines in human sequence are marked. Respective GenBank accession numbers are: NP_996986, XP_849038, NP_001038991, XP_001251000, and XP_001377777. Sequence of *Danio rerio* SCIMP was deduced from two overlapping expressed sequence tag (EST) sequences, EB765140 and EB768085 (C) RT-qPCR analysis of SCIMP mRNA expression in human tissues. Average expression in all tissues corresponds to value 1 on the vertical axis. Data are presented as the mean of four experiments (± SD). (D) Western blot reactivity of anti-SCIMP antibodies on lysates from nontransfected B cell lines Ramos (human) and K46 (murine) or from HEK293 cells transfected with human (hSCIMP) or murine SCIMP (mSCIMP) constructs or empty vector. hSCIMP was stained with mouse monoclonal antibody (NVL-07) and mSCIMP with rabbit antiserum to mSCIMP. (E) SCIMP expression in mouse tissues and peripheral blood leukocytes (PBLs), analyzed by immunoblotting. (F) SCIMP and MHC-II expression in isolated human blood leukocyte subsets and in monocyte-derived dendritic cells (MDDC), analyzed by immunoblotting. GAPDH serves as a loading control; data are representatives of two independent experiments (E and F).

established Csk-binding partners, including PAG and LIME, we identified an unknown polypeptide (145 aa long in humans), termed c17orf87. As mentioned above, we renamed this protein SCIMP. It possesses features typical of TRAPs. A short leaderless extracellular domain is followed by a predicted transmembrane domain, a potential palmitoylation (S-acylation) motif (CXC), and a larger cytosolic tail containing four potential tyrosine phosphorylation sites that may interact with SH2 domains (Fig. 1A). A putative binding site for Csk is represented by Y_{107}SLV sequence. Y_{69}ENV sequence is a typical binding site for Grb2 family adaptor proteins (19, 35). Y_{131}DDV sequence is a predicted motif for binding to the adaptor proteins SLP65 and SLP76 (17, 44). In addition, SCIMP contains a proline-rich sequence, a likely binding site for Src homology 3 (SH3) domains (32) (Fig. 1A).

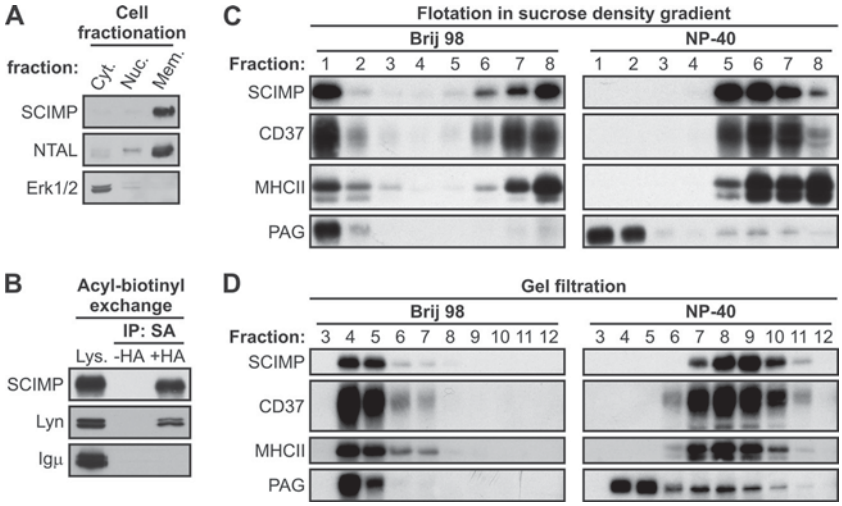

FIG. 2. SCIMP is a palmitoylated transmembrane protein present in Brij 98- but not NP-40-resistant membrane microdomains. (A) Fractionation of Ramos cells into cytoplasmic (Cyt.), nuclear (Nuc.), and membrane (Mem.) fractions, followed by SCIMP immunoblotting. NTAL and Erk2 staining served as controls for membrane and cytoplasmic fractions, respectively. (B) Acyl-biotinyl exchange reaction performed on lysates (Lys.) from membrane fractions of Ramos cells. Non-hydroxylamine-treated samples (−HA) served as a negative control, while HA treatment (+HA) allowed exchange of palmitate for biotin moiety and isolation of palmitoylated proteins on immobilized streptavidin. Lyn and Igμ staining, respectively, served as positive and negative controls for specificity of isolation. (C and D) Brij 98 or NP-40 lysates from Ramos cells were fractionated by flotation in sucrose density gradient (C) or by gel filtration on Sepharose 4B (D). Samples were analyzed for distribution of SCIMP, CD37, MHC-II, and PAG. Data are representative of two independent experiments.

To detect evolutionarily conserved regions in SCIMP, we employed the Basic Local Alignment Search Tool (BLAST) at NCBI (http://blast.ncbi.nlm.nih.gov/Blast.cgi) to search for SCIMP homologues from different vertebrate species in GenBank nucleotide and protein databases, including genomic and expressed sequence tag (EST) collections. We identified SCIMP in a number of mammals and in zebrafish. The alignment of a representative selection of SCIMP sequences revealed that the SCIMP typical domain organization of a TRAP is conserved throughout evolution (Fig. 1B). Only two of the predicted protein interaction motifs were preserved in all species analyzed: the putative SLP65/SLP76 interaction motif (duplicated in zebrafish) and the proline-rich sequence.

Expression of SCIMP in antigen-presenting cells. We investigated the expression of human SCIMP in various tissues at the mRNA level and observed the strongest expression in lymph nodes and spleen (Fig. 1C), whereas only a negligible amount of SCIMP mRNA was detected in the majority of nonimmune system tissues.

Subsequently, we generated both mouse monoclonal antibodies and rabbit antisera against the cytoplasmic part of human SCIMP, as well as rabbit antisera against the cytoplasmic part of mouse SCIMP, which detected an endogenous protein with an apparent molecular mass of ~20 kDa in murine and human B cell lines (Fig. 1D and data not shown). The size is somewhat higher than that predicted from SCIMP sequence (17 kDa). However, the same mobility was also observed for SCIMP expressed from the cDNA construct in HEK293 cells, suggesting unusual electrophoretic mobility of this polypeptide (Fig. 1D). We used the antibodies to analyze expression of SCIMP at the protein level in mice. Western blot analysis of various organs and tissues revealed an expression pattern similar to that observed before at the mRNA level in human tissues. A large amount of the SCIMP protein was detected in the spleen and lymph nodes and a low level in other tissues of the immune system, including bone marrow, peripheral blood leukocytes (PBLs), and thymus; a lack of SCIMP expression was again confirmed in the majority of nonimmune tissues, with the exception of lung (Fig. 1E).

To assess SCIMP expression in individual leukocyte subpopulations, we purified different leukocyte subsets from human blood. Peripheral blood monocyte-derived dendritic cells (MDDCs) were also included. Interestingly, we observed a significant amount of SCIMP just in professional APCs, namely, B cells, monocytes and MDDCs, whereas only negligible to no amounts of SCIMP were detected in other cell types. Accordingly, the expression of SCIMP correlated with that of MHC-II in these samples (Fig. 1F).

Subcellular distribution and palmitoylation of SCIMP. The SCIMP sequence contains a predicted transmembrane domain followed by a potential palmitoylation motif. Indeed, the majority of SCIMP was recovered from the membrane fraction of Ramos B cells (Fig. 2A). Moreover, using an acyl-biotinyl exchange assay (48), a method based on the exchange of palmitoyl residues in proteins for the biotin moiety, we demonstrated that SCIMP is palmitoylated (Fig. 2B), likely at one or both of the cysteines within the potential submembrane palmitoylation motif, since these are the only cysteines in the human SCIMP sequence. It should be noted that this method cannot distinguish between palmitoylation and other, much rarer types of protein S-acylation involving different fatty acyl residues. On the other hand, it detects neither N-terminal myristoylation nor C-terminal prenylation. However, for these modifications, SCIMP does not contain consensus sequences.

Palmitoylation is one of the prerequisites for protein targeting to membrane microdomains, such as lipid rafts. One of the characteristic features of these domains is their resistance to solubilization in particular detergents (8). To verify whether

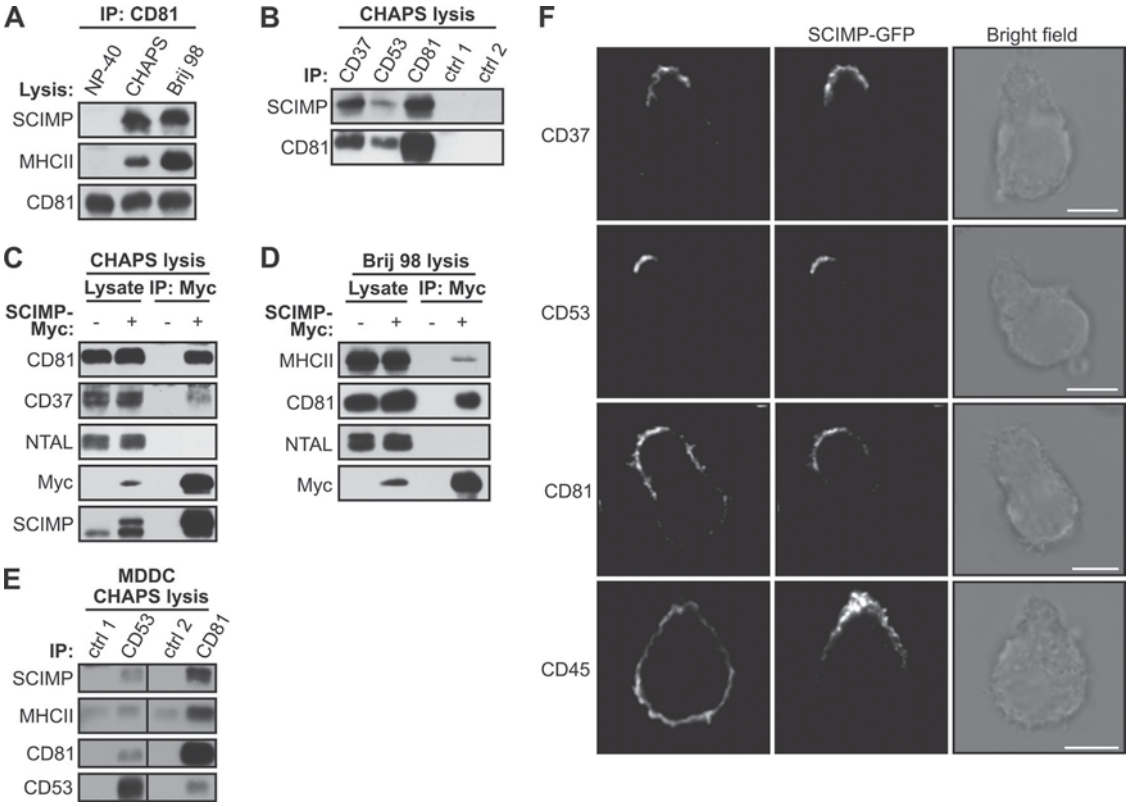

FIG. 3. Localization of SCIMP in tetraspanin-enriched microdomains. (A) NP-40, CHAPS, or Brij 98 lysates from Ramos cells were immunoprecipitated with anti-CD81 antibody, and samples were stained for SCIMP, MHC-II, and CD81. (B) CHAPS lysates of Ramos cells were immunoprecipitated with anti-CD37, anti-CD53, anti-CD81, or isotype control antibodies, followed by staining for SCIMP and CD81. (C and D) CHAPS (C) or Brij 98 (D) lysates of Ramos cells transfected with SCIMP-Myc or empty vector were immunoprecipitated with anti-Myc antibody, and samples were stained as indicated. (E) CHAPS lysates of human monocyte-derived dendritic cells (MDDC) immunoprecipitated with isotype control antibodies, followed by immunoprecipitation with anti-CD53 or anti-CD81, were stained for SCIMP, MHC-II, CD81, and CD53. (F) Spontaneously polarized Ramos cells transfected with SCIMP-GFP were stained for CD37, CD53, CD81, or control CD45 and analyzed by confocal microscopy. Scale bar = 5 μm. Data are representative of two (A and F) or three (B, C, and D) independent experiments.

SCIMP is localized in lipid rafts, we solubilized Ramos cells in Brij 98- or NP-40-containing lysis buffers and fractionated the resulting lysates using flotation in a sucrose density gradient. About half of SCIMP was present in the low-density fractions when a mild detergent, Brij 98, was used, but upon solubilization in the more stringent detergent NP-40, SCIMP was recovered only from bottom fractions of the gradient (Fig. 2C). This was in marked contrast to the raft resident protein PAG (6), which was recovered from low-density fractions in both detergents, demonstrating that SCIMP is not localized in classical lipid rafts determined to be microdomains resistant to TX-100-related detergents, such as NP-40. Interestingly, tetraspanin CD37, as well as tetraspanin-associated MHC-II (3), exhibited a behavior similar to that of SCIMP (Fig. 2C). Moreover, upon fractionation of cell lysates by gel filtration on Sepharose 4B, SCIMP was recovered in large detergent-resistant complexes upon lysis in Brij 98 but was completely solubilized in NP-40. Again, this behavior was markedly different from that of NP-40-resistant PAG containing microdomains but resembled the behavior of tetraspanin CD37 and of MHC-II (Fig. 2D).

Association of SCIMP with TEMs. Similar solubility profiles of SCIMP and tetraspanin proteins led us to hypothesize that SCIMP could be a constituent of TEMs (49). To test this idea, we performed a series of immunoprecipitation experiments. First we lysed Ramos cells in buffers containing Brij 98, CHAPS, or NP-40 detergents and immunoprecipitated tetraspanin CD81. Upon solubilization of cells in Brij 98 or CHAPS, detergents that preserve TEMs (4, 42), we detected an interaction between CD81 and both MHC-II and SCIMP (Fig. 3A). These associations were completely lost upon solubilization in the tetraspanin-disrupting detergent NP-40. Furthermore, SCIMP coimmunoprecipitated with CD37, CD53, and CD81 after solubilization of cells in CHAPS (Fig. 3B). We also detected an interaction of CD81 with CD37 and CD53, proving that the integrity of TEMs was not compromised.

Next, we prepared Ramos cells virally infected with a vector coding for Myc-tagged SCIMP (SCIMP-Myc) or an empty vector. Upon solubilization of cells in CHAPS, it was possible to specifically coimmunoprecipitate CD37 and CD81 with SCIMP-Myc (Fig. 3C); however, no interaction with a lipid raft marker, NTAL (25), was observed; this further confirms that SCIMP is not a component of lipid rafts (Fig. 3C). When the same experiment was performed with Brij 98 cell lysates, a weak interaction was detectable between SCIMP-Myc and MHC-II, but the binding of SCIMP-Myc to CD81 was much stronger (Fig. 3D). This suggests that while the interaction with

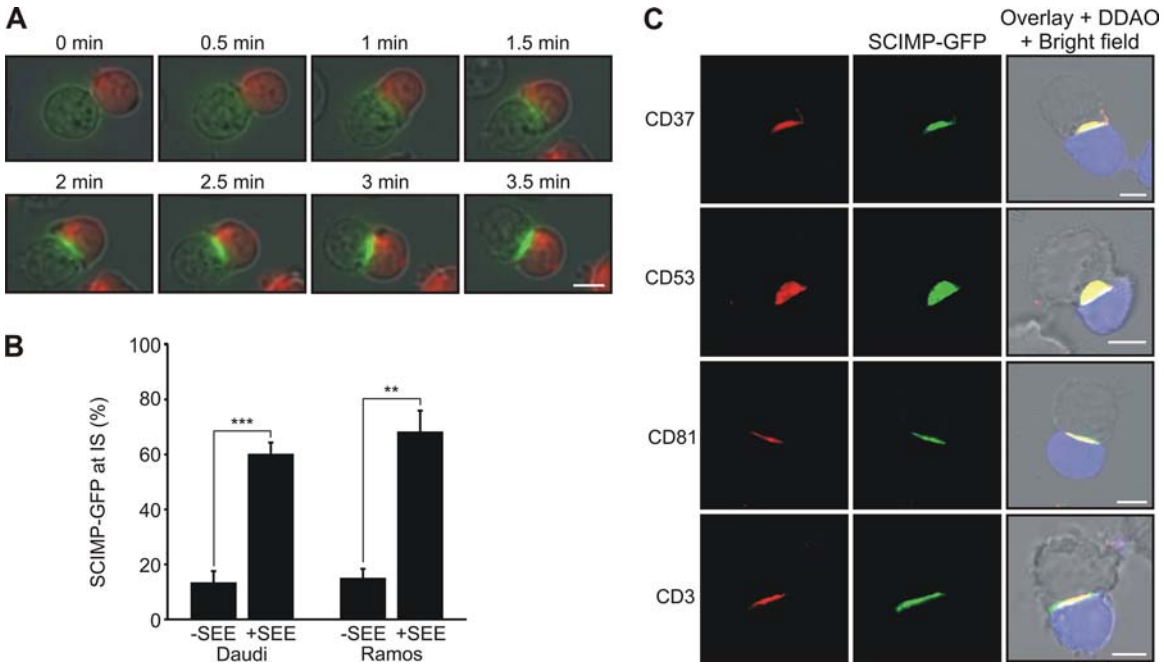

FIG. 4. Translocation of SCIMP into immunological synapse. (A) Ramos cells transfected with SCIMP-GFP (green) were loaded with superantigen, and subsequently Jurkat T cells (labeled by DDAO in red) were added. Immunological synapse formation was observed by live cell imaging. (B) Daudi or Ramos cells transfected with SCIMP-GFP were loaded (+SEE) or not (−SEE) with superantigen, and Jurkat cells were added. The percentage of cells with SCIMP-GFP translocated to the cell-cell contact is shown. Results are means ± SD from three independent experiments; at least 100 conjugates were analyzed in each experiment. **, $P < 0.01$; ***, $P < 0.001$ (two-tailed Student test with assumed nonequal variances). (C) Ramos cells transfected with SCIMP-GFP were loaded with superantigen and mixed with Jurkat T cells labeled with DDAO (in blue). After IS formation, cells were fixed and stained for CD37, CD53, CD81, or CD3 and analyzed by confocal microscopy. Scale bar = 5 μm. Data are representative of two independent experiments.

some of the tetraspanins may be direct, binding to MHC-II is likely to be indirect, perhaps mediated by members of the tetraspanin family. Finally, we also could coimmunoprecipitate both SCIMP and MHC-II with CD37 and CD81 from CHAPS lysates of human MDDC, thus proving that this interaction can also be detected in primary cells (Fig. 3E).

Tetraspanins and tetraspanin-associated proteins have been observed in the uropod of migrating cells (43). To characterize the localization of SCIMP in polarized cells, we transfected the Ramos cell line with SCIMP fused to C-terminal GFP. Interestingly, a fraction of Ramos cells displayed a migratory morphology with a well-distinguished leading edge and uropod. In these cells, a vast majority of SCIMP colocalized with tetraspanins CD37, CD53, and CD81 in the uropod (Fig. 3F). Together these results provide strong evidence at biochemical and microscopic levels for an association of SCIMP with TEMs.

SCIMP localization to IS. Thus far, we have demonstrated that SCIMP is a part of MHC-II-containing TEMs. Some of the tetraspanins have been shown to partition to the IS between the APC and the T cell (34). To find out whether SCIMP may also localize to the IS, we used Ramos and Daudi B cell lines expressing SCIMP-GFP as APCs in a superantigen staphylococcal enterotoxin E (SEE)-based assay. Live-cell imaging of superantigen-induced conjugates between SCIMP-GFP-expressing Ramos or Daudi cells and the Jurkat T cell line revealed that early after conjugate formation, SCIMP was rapidly translocated into the IS (Fig. 4A and B; see also video S1 in the supplemental material). Similar behavior was also observed for several tetraspanin molecules, including CD37, CD53, and CD81 (Fig. 4C). These studies strongly suggest a connection between SCIMP and processes originating at the APC side of the IS.

Phosphorylation of SCIMP upon MHC-II cross-linking. Expression of SCIMP in APCs and localization in TEMs together with MHC-II and clustering of SCIMP at the IS implied that SCIMP may be involved in signaling pathways resulting from engagement of MHC-II molecules during antigen recognition. To determine whether the engagement of MHC-II molecules could possibly influence SCIMP phosphorylation, we therefore isolated mouse splenic B cells, stimulated them with either anti-BCR or anti-MHC-II antibodies, and subsequently isolated SCIMP via immunoprecipitation. Compared to BCR activation, MHC-II molecule cross-linking induced only a mild increase in overall tyrosine phosphorylation (Fig. 5A). However, stimulation with anti-MHC-II led to a marked increase in SCIMP tyrosine phosphorylation, whereas BCR activation had no effect on phosphorylation of SCIMP (Fig. 5B).

After MHC-II stimulation, both Src and Syk family kinases are activated (1). To determine the kinases responsible for phosphorylation of SCIMP, we cotransfected HEK293 cells with Syk, Lyn, Src, Fyn, or empty vector together with either SCIMP or NTAL. In contrast to the established Syk substrate NTAL (25), SCIMP was most strongly phosphorylated by Lyn and Src, while Syk had no effect (Fig. 5C). Based on these findings, we conclude that Src, but not Syk, family kinases are

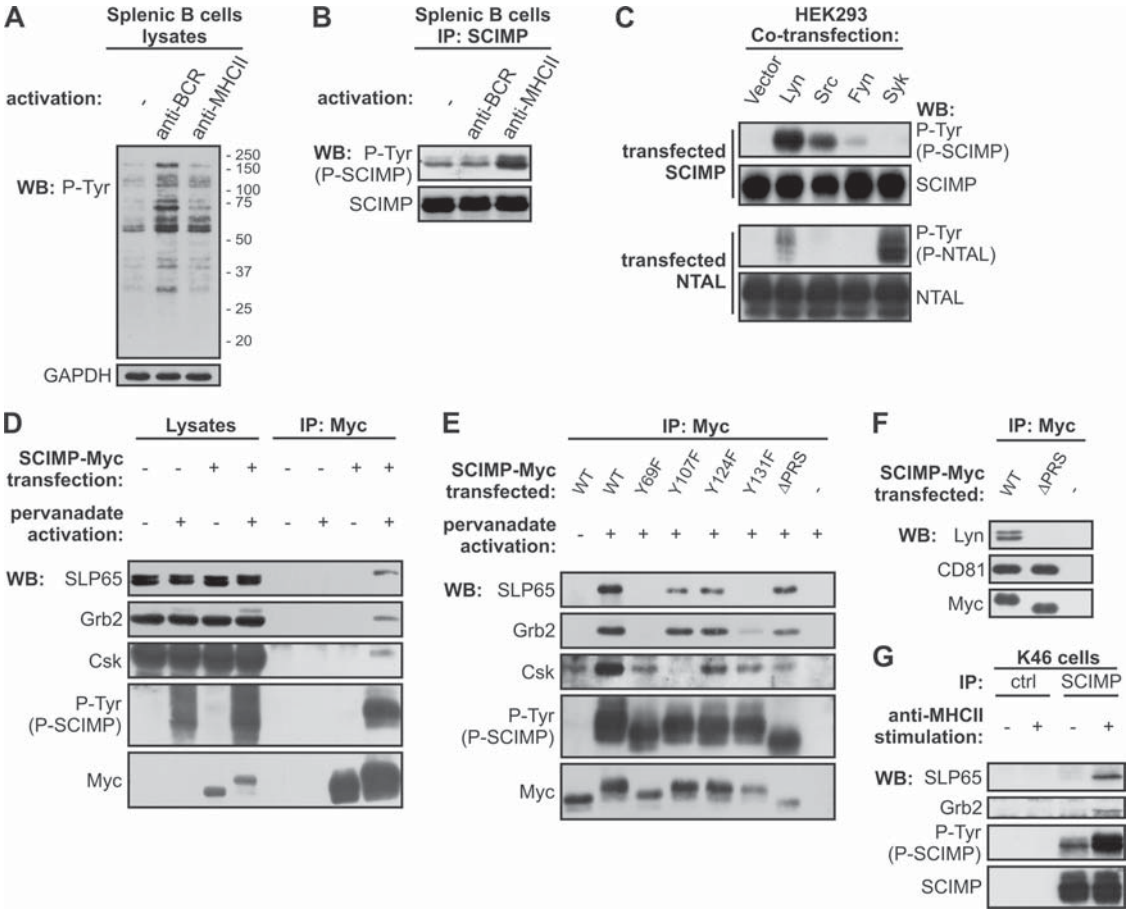

FIG. 5. SCIMP is phosphorylated upon MHC-II stimulation and binds Grb2-SLP65 complex, Csk, and Lyn. (A) Isolated splenic B cells were left untreated (−) or activated with anti-BCR or anti-MHC-II antibodies for 2 min and lysed in laurylmaltoside, and whole-cell lysates were analyzed by antiphosphotyrosine staining. GAPDH served as a loading control. (B) Isolated splenic B cells were treated as for panel A, SCIMP was immunoprecipitated, and samples were probed for phosphorylated SCIMP (P-Tyr) or for total SCIMP. (C) HEK293 cells were cotransfected with SCIMP or NTAL together with either empty vector or plasmids coding for Lyn, Src, Fyn, or Syk kinases. Phosphorylation of SCIMP or NTAL was analyzed by antiphosphotyrosine staining. (D) Ramos cells transfected with SCIMP-Myc or empty vector were stimulated or not with pervanadate and lysed in laurylmaltoside, and SCIMP-Myc was immunoprecipitated. Samples were probed with SLP65, Grb2, Csk, Myc, and phosphotyrosine (P-Tyr) antibodies. (E) Ramos cells transfected with either wild-type (WT) SCIMP-Myc, SCIMP-Myc with indicated tyrosines mutated to phenylalanines, or SCIMP-Myc containing deletion of proline-rich sequence (ΔPRS) were treated as for panel D. (F) Ramos cells transfected with WT SCIMP-Myc or ΔPRS SCIMP-Myc were lysed in Brij 98, and SCIMP-Myc was immunoprecipitated. Samples were stained for Myc, Lyn, and CD81. (G) K46 cells were left untreated or activated with anti-MHC-II antibody, lysed in laurylmaltoside, and immunoprecipitated with antisera to SCIMP or preimmune control sera. Samples were probed for phosphorylated SCIMP using antiphosphotyrosine antibody and for total SCIMP, SLP65, and Grb2. Data are representatives of two (A, B, and C) or three (D to G) independent experiments.

likely to be responsible for the phosphorylation of SCIMP upon MHC-II cross-linking.

SCIMP interaction with SLP65/SLP76, Grb2, Csk, and Lyn. Phosphorylated SCIMP may serve as a binding platform for SH2 domains of several proteins, as deduced from sequence analysis. To verify the predicted binding partners, we first induced strong protein phosphorylation by treating SCIMP-Myc-transfected Ramos cells with pervanadate (PV), a potent inhibitor of protein tyrosine phosphatases, and lysed the cells with a relatively stringent detergent, laurylmaltoside. Subsequently, SCIMP-Myc was immunoprecipitated with anti-Myc antibody. Upon PV treatment, SCIMP became strongly phosphorylated, and we could easily detect interactions of SCIMP with the SLP65, Grb2, and Csk proteins in these immunoprecipitates (Fig. 5D). Interestingly, even though SLP65 is expressed in two isoforms, SCIMP interacted only with the longer form, which contains a binding site for the SH3 domain of Grb2 (18). This implies that binding of SLP65 to SCIMP may require the formation of a trimolecular complex involving Grb2.

In order to identify the phosphorylation sites responsible for binding of these signaling molecules, we mutated all individual tyrosines in the intracellular part of SCIMP-Myc to phenylalanines. In addition, we also deleted the proline-rich sequence between aa 81 and 104. We treated transfected cells with PV and immunoprecipitated SCIMP-Myc. As expected, mutation of Y107 led to the loss of Csk binding capacity (Fig. 5E). Moreover, mutation of either of the predicted binding sites for Grb2 and SLP65, Y69 and Y131, respectively, resulted in a simultaneous loss of binding of both adaptors to SCIMP (Fig. 5E). These studies suggest a level of cooperativity in the interaction among SCIMP, SLP65, and Grb2. It was also possible to

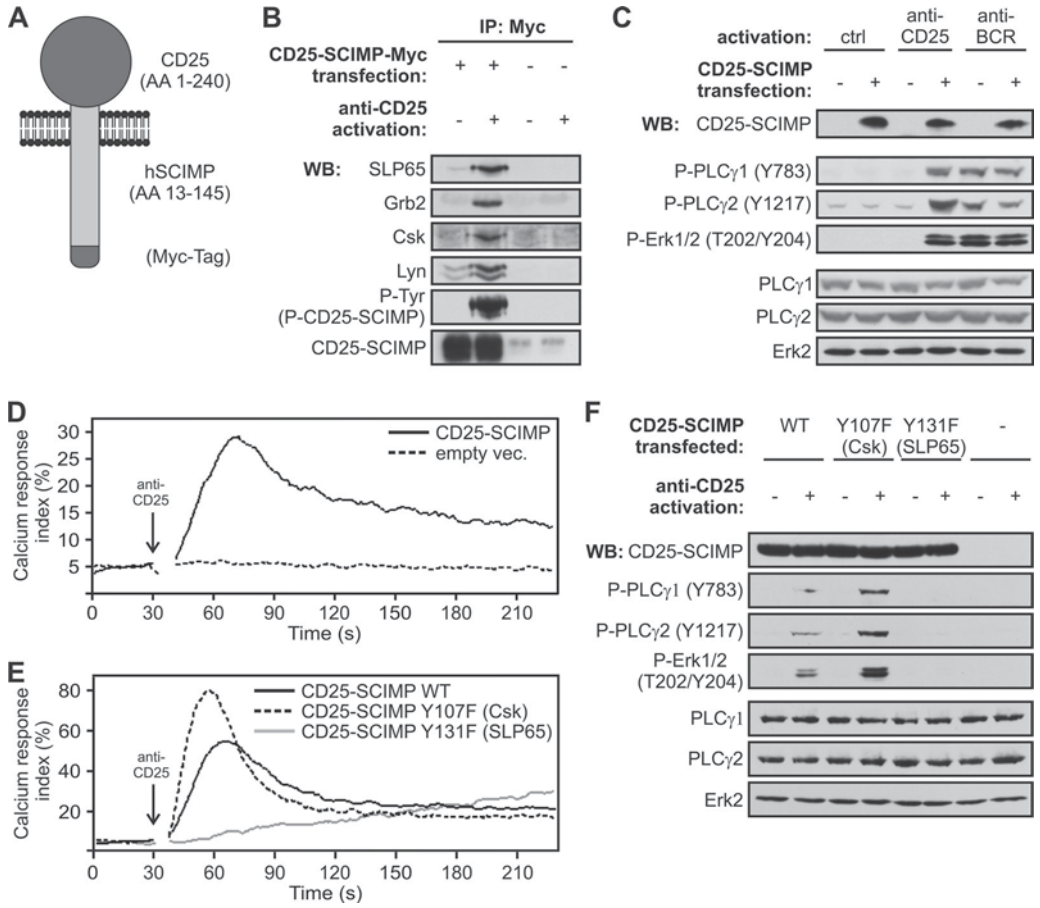

FIG. 6. Cross-linking of SCIMP initiates signaling events. (A) Schematic representation of CD25-SCIMP chimera containing or not containing a Myc tag. (B) Raji cells transfected with CD25-SCIMP-Myc or empty vector were activated (or not) with anti-CD25 antibody, lysed in laurylmaltoside, immunoprecipitated with anti-Myc antibody, and stained with SLP65, Grb2, Lyn, Csk, SCIMP, and phosphotyrosine antibodies (band corresponding to CD25-SCIMP is shown). (C) Raji cells transfected with CD25-SCIMP or empty vector were activated for 5 min or not by anti-CD25 or anti-BCR antibody, and samples were stained as indicated. (D) Calcium response of Raji cells transfected with CD25-SCIMP or empty vector after CD25 cross-linking. (E) Calcium response after CD25 cross-linking in Raji cells transfected with a CD25-SCIMP-Myc chimera containing either WT sequence of SCIMP or SCIMP with indicated tyrosine-to-phenylalanine mutations (Y107F [Csk binding site] or Y131F [SLP65 binding site]). (F) Raji cells transfected with CD25-SCIMP-Myc chimeric constructs coding for WT or tyrosine mutants of SCIMP or with empty vector were activated with anti-CD25 antibodies and stained as indicated. Data (B to F) are representative of two independent experiments.

detect an interaction of SCIMP with the Src family kinase Lyn after cell solubilization in a mild detergent, Brij 98 (Fig. 5F). The constitutive nature of this association implies that it might be based on interactions between the proline-rich sequence of SCIMP and the SH3 domain of Lyn. Indeed, deletion of the proline-rich sequence of SCIMP abolished this association (Fig. 5F). Similar interactions were also observed in the myeloid cell line THP1, except that SLP76 was the predominant member of the SLP adaptor family detected in SCIMP immunoprecipitates (not shown).

Finally, these data were confirmed in an experiment with endogenous proteins from nontransfected cells using only MHC-II stimulation. Murine B cell line K46, a well-established model for MHC-II signaling (31), was stimulated with anti-MHC-II antibody, and SCIMP was immunoprecipitated from the corresponding cell lysates. SLP65 and Grb2 coimmunoprecipitated with SCIMP (Fig. 5G), but no Csk or Lyn could be detected in these samples. Since SCIMP is a very small protein, it is possible that our anti-SCIMP antibodies competed with Csk and Lyn for binding to SCIMP.

Cross-linking of CD25-SCIMP fusion protein results in multiple signaling events. The results indicate that SCIMP may be involved in signal transduction events initiated by MHC-II/SCIMP aggregation at the IS. MHC-II glycoproteins are known to trigger multiple signaling pathways employing a range of coreceptors and adapter molecules. Thus, it was essential to find out which of these pathways can be directly regulated by SCIMP and can be attributed to its association with SLP family adaptors and other binding partners. To address this, we prepared a fusion construct composed of the extracellular portion of human CD25 followed by the human SCIMP sequence (starting at S_{13}) and a Myc tag for immunoprecipitation studies at the C terminus (Fig. 6A). Transduction of the CD25-negative B cell line Raji with this construct resulted in surface expression of the CD25-Nvl chimera at an expression level comparable to that of endogenous SCIMP in

these cells (not shown). We cross-linked the CD25-SCIMP fusion protein on the surface of these cells by CD25-specific antibody. Immunoprecipitation of CD25-SCIMP then revealed a significant increase in CD25-SCIMP phosphorylation and also induced an association with Csk, SLP65, and Grb2 and surprisingly with Lyn as well (Fig. 6B).

Since aggregation of SCIMP led to its association with potential effector molecules, we decided to find out whether it would also initiate the downstream effector pathways. After CD25-SCIMP cross-linking, we observed a strong increase in phosphorylation of PLC-γ1 and PLC-γ2 (Fig. 6C), accompanied by an intracellular calcium increase (Fig. 6D). Moreover, when looking at further downstream events, we detected a significant increase in phosphorylation of the MAPK Erk1/2, comparable to the levels of phosphorylation induced by BCR (Fig. 6C).

In order to specify which of the SCIMP-associated molecules are involved in the regulation of these events, we generated CD25-SCIMP-Myc chimeras where tyrosines Y107 (Csk binding site) and Y131 (SLP65 binding site) were mutated to phenylalanines, and we transfected these constructs into Raji cells at similar expression levels (not shown). Strikingly, mutation of the SLP65 binding site almost completely abolished the calcium response downstream of CD25-SCIMP chimeras, while mutation of the Csk binding site had a strong enhancing effect (Fig. 6E). In agreement with this result, no increase in phosphorylation of PLC-γ1, PLC-γ2, or Erk1/2 could be detected after cross-linking of the chimeras with the mutated SLP65 binding site. In contrast, hyperphosphorylation of these molecules was observed after mutating the tyrosine responsible for binding to Csk (Fig. 6F). These data strongly suggest that SCIMP can initiate and propagate signaling by recruiting SLP65 and that it is regulated via the recruitment of Csk.

SCIMP is required for sustained Erk signaling upon MHC-II stimulation. All the data obtained so far indicate that SCIMP is directly involved in propagation of signaling from MHC-II molecules, mainly by recruiting the SLP65 adaptor protein. However, this adaptor also binds to Igα/β heterodimers (38) known to be involved in MHC-II signal transduction, and there may also be other, less well defined mechanisms of its membrane recruitment dependent on its N-terminal region. In order to find out if there is any nonredundant role for SCIMP and SCIMP-associated SLP65 in MHC-II signal transduction, we infected the K46 murine B cell line with lentiviruses carrying vectors coding for mouse SCIMP-specific shRNAs. Infections with viruses coding shRNA 1 and shRNA 3 resulted in a more than 90% downregulation of SCIMP, while the vector coding nonsilencing shRNA 2 and the empty vector served as negative controls (Fig. 7A and B). Two clones were selected from each transfected cell line to avoid the risk of clonal bias. After activation of these cell lines via MHC-II molecule cross-linking, no effect of SCIMP downregulation on calcium response was observed (not shown). On the other hand, sustained activity of the Erk pathway was strongly affected by SCIMP deficiency. Only a transient Erk1/2 phosphorylation was detectable in SCIMP-deficient cell lines, with a marked reduction at the 10-min time point (Fig. 7A and B). Importantly, this effect was observed across the entire Erk pathway, since other components of this pathway, MEK1/2 (activator of Erk1/2) and p90RSK (Erk1/2 downstream target), were similarly affected (Fig. 7A and B).

To examine the effect of SCIMP-associated SLP65 and Csk on this pathway, we performed a knockdown rescue experiment in which two K46 clones expressing shRNA 3 were retrovirally infected with vectors coding for wild-type human SCIMP or human SCIMP with a mutated Csk binding site (Y107F) or SLP65 binding site (Y131F) and with a control empty vector. Note that the human SCIMP constructs would not be affected by mouse shRNA 3 sequences. Ten minutes after MHC-II molecule stimulation, cells expressing wild-type human SCIMP exhibited increased Erk1/2 phosphorylation compared to the control. An even stronger effect was observed when the Csk binding site was mutated (Fig. 7C and D). In contrast, cells transfected with the human SCIMP mutant unable to bind SLP65 were incapable of sustaining Erk1/2 phosphorylation. Again, the same applied for activation of MEK1/2 and p90RSK. Together, these data strongly suggest that SLP65 binding to SCIMP is necessary for sustained Erk1/2 signaling downstream of MHC-II molecules. Concomitant binding of Csk serves as a negative regulatory loop to modulate the SCIMP function.

DISCUSSION

TRAPs are implicated as regulators and/or organizers of signaling from various plasma membrane receptors. Expression of some of them, like PAG, is ubiquitous, indicating that they have a general role in cells of various origins (6), while others, such as LAT, are expressed in a highly tissue-restricted pattern, pointing toward a more specific role. Indeed, LAT is present mainly in T cells, NK cells, and mast cells and functions as a critical regulator of TCR and Fc receptor signaling (21). Analysis of SCIMP expression revealed its presence to be strictly limited to tissues of the immune system, most prominently in the lymph nodes and spleen. Probing this further, we observed a clear correlation between the expression of SCIMP and MHC-II molecules in APCs. This suggested that the functions of SCIMP may be coupled to the regulation of antigen presentation or APC activation.

SCIMP contains a transmembrane domain followed by palmitoylated (S-acylated) cysteines. It should be noted that even though most S-acylated proteins contain palmitate, other fatty acid residues have also been detected, such as palmitoleate, stearate, oleate, arachidonate or eicosapentanoate (36, 39). In contrast to other palmitoylated TRAPs (LAT, NTAL, LIME, and PAG), SCIMP is not found in "classical" lipid rafts. Instead, we provided biochemical evidence that SCIMP is associated with tetraspanins CD37, CD53, and CD81 and established SCIMP as a novel constituent of TEMs.

Current knowledge of TEM function in antigen presentation is rather limited. MHC-II molecules loaded with specific antigenic peptides appear to be enriched in TEMs (30, 47), and it has been suggested that TEMs might increase the chance of successful presentation of a limited pool of MHC-II molecules loaded with specific peptides. This would be in agreement with the observation that tetraspanins are constituents of IS (34). SCIMP is also rapidly translocated to IS. Since SCIMP contains only a very short extracellular part, this process is most likely mediated through interaction with TEMs.

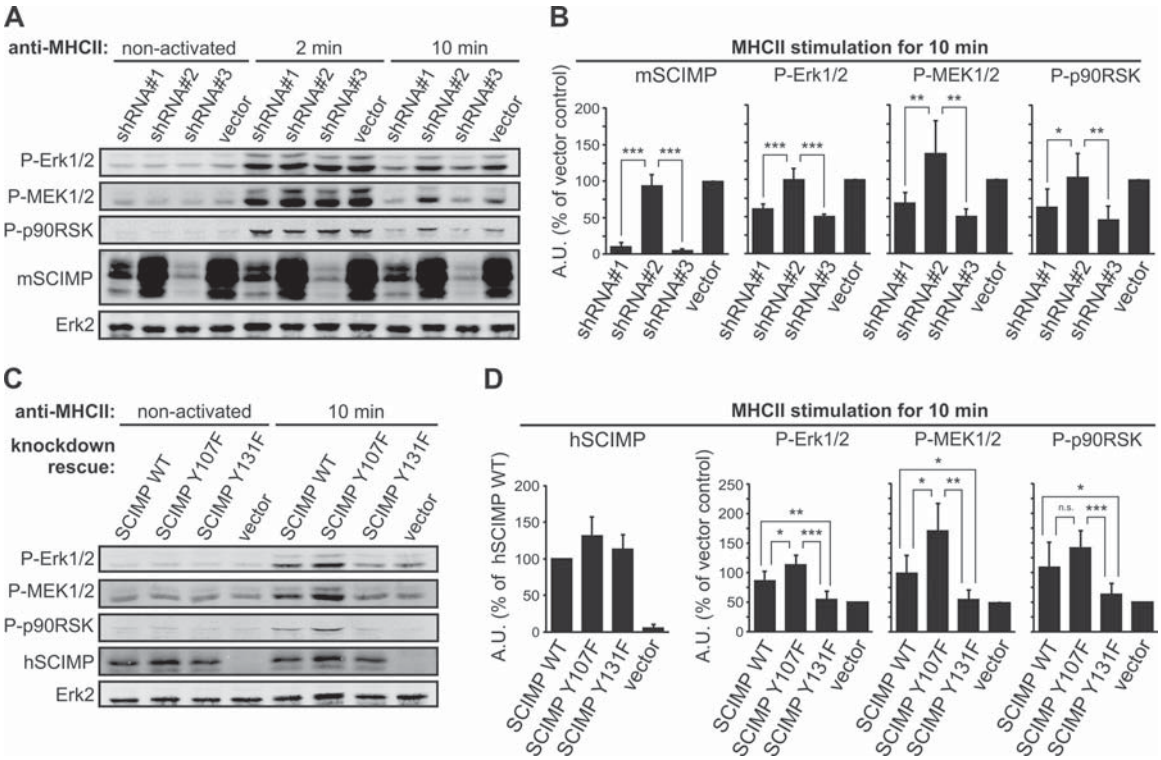

FIG. 7. SCIMP mediates sustained Erk signaling after MHC-II-mediated activation. (A) K46 murine B cells were lentivirally infected with vectors coding for shRNAs against SCIMP or with empty vector. While shRNA 1 and shRNA 3 mediated strong knockdown, shRNA 2 served as a control. Cells were activated with anti-MHC-II antibodies for indicated times and analyzed for phosphorylation of Erk1/2 (T202/Y204), MEK1/2 (S217/221), and p90RSK (S380) or for expression of mSCIMP. Total Erk2 staining served as a loading control. (B) Statistical analysis of results in panel A from six independent experiments using two clones from each cell line. Samples were normalized to the loading control (means ± SD). (C) Clones expressing shRNA 3 were reconstituted with wild-type (WT) human SCIMP or with human SCIMP with a mutated Csk binding site (Y107F) or SLP65 binding site (Y131F) or with empty vector. Cells were activated and analyzed as described for panel A, with staining for transfected human SCIMP added. (D) Statistical analysis of results in panel C from six independent experiments using two clones from each cell line. Samples were normalized to the loading control (means ± SD). *, $P < 0.05$; **, $P < 0.01$; ***, $P < 0.001$ (two-tailed Student test with assumed nonequal variances). All data were collected using the Odyssey infrared imaging system. A.U., arbitrary units.

Even though the role of signals generated by interactions with MHC-II molecules is still rather unclear, there is ample evidence that MHC-II molecules are not just passive tools to display peptides on the cell surface. Responses generated via MHC-II molecule ligation range from APC activation and differentiation to apoptosis. Engagement of MHC-II on the APC surface using specific antibodies results in activation of Src and Syk family kinases, induction of calcium influx, and activation of MAPKs, protein kinase C (PKC) family members, and the phosphatidylinositol 3-kinase (PI3K)-Akt pathway, as well as downstream activation of transcription factors NF-AT and AP1 (1, 20). The key question is how the signaling by MHC-II molecules is initiated, since MHC-II molecules possess only short cytoplasmic parts without any apparent signaling motifs. Signaling mechanisms of MHC-II glycoproteins were studied mainly in B cells, where MHC-II interactions with Igα/β, CD19, or MPYS were suggested to be involved in mediating the signal transmission (5, 26, 31), but the precise pathways and number of key players still remain incompletely defined. Here we have identified SCIMP as one of possible mediators of MHC-II molecule signal transduction. In splenic B cells, SCIMP phosphorylation substantially increased after MHC-II cross-linking but not after BCR cross-linking. The SCIMP signaling capacity probably depends to a large extent on phosphorylation of the tyrosine motifs in its intracellular domain. Based on the current knowledge of SH2 domain binding preferences, it was possible to predict and confirm by coimmunoprecipitation the binding partners for three of these tyrosines (Grb2 for Y_{69}, Csk for Y_{107}, and SLP65/SLP76 for Y_{131}). It should be noted that the list of binding partners for phosphorylated SCIMP might be incomplete, and some other, so far unknown proteins could bind via their SH2 domains to phosphorylated SCIMP in a competitive manner.

We observed a high level of cooperativity in SLP65/SLP76 and Grb2 binding to SCIMP. It has been shown that both SLP65 and SLP76 interact via their proline-rich motifs with the SH3 domain of Grb2 (15, 24), thereby forming a complex where both proteins have SH2 domains available for binding. We suggest that this "bivalent" mode of binding would substantially increase the avidity of the interaction between Grb2, SLP65/SLP76, and SCIMP.

Binding of SCIMP to both Lyn and Csk is reminiscent of findings for LIME and PAG (6, 7). These adaptors also bind both the Src family kinases and Csk and are mainly considered negative regulators, since they anchor the inhibitory Csk in lipid rafts. However, binding of SCIMP to SLP65/SLP76 adap-

tors also suggests an active role for SCIMP in signal transduction. To better understand the dual activatory/inhibitory nature of this adapter and its direct effect on signaling pathways, we generated the CD25-SCIMP chimeric protein. Direct cross-linking of this construct led to increased CD25-SCIMP phosphorylation and concomitant binding of the SLP65/SLP76-Grb2 complex and Csk kinase. The overall functional outcome of CD25-SCIMP cross-linking was activation of several signaling pathways, including phosphorylation of PLC-γ1 and PLC-γ2, a robust calcium response, and Erk1/2 activation. Since we did not observe a direct association between SCIMP and PLC-γ isoforms (not shown), the signal events initiated by cross-linking of CD25-SCIMP were most likely mediated by anchoring SLP65 to the plasma membrane. SLP65 could associate there with various effector proteins, such as PLC-γ isoforms and their activator, Btk (28). This hypothesis is corroborated by the observation that all signaling pathways emanating from CD25-SCIMP were abolished by mutation of the SLP65/SLP76 binding site. Notably, the BCR signaling subunit Igα also contains a SLP65 binding tyrosine, and its mutation compromises the BCR signaling pathway (13, 38).

An opposite phenotype was observed when the Csk-binding tyrosine was mutated, since all the responses generated after cross-linking of CD25-SCIMP were substantially enhanced, indicating a direct role of Csk in the regulation of signaling mediated by SCIMP. These results lead to important conclusions. First, SCIMP has an overall activating function dependent on SLP65 binding, and interaction with Csk is employed to modulate SCIMP's own activity. Second, among the many responses elicited by MHC-II stimulation, SCIMP is directly involved in generating the calcium response and enhancing Erk1/2 activity.

A complementary approach to provide evidence for the signaling capabilities of SCIMP was the generation of K46 cell lines with diminished expression of SCIMP. Surprisingly, we observed no effects on the calcium response after MHC-II molecule cross-linking. This observation does not rule out the role of SCIMP in the calcium response, but combined with our results with CD25-SCIMP chimeras it rather suggests that MHC-II-dependent calcium signaling may be under the control of multiple redundant pathways. In contrast, the Erk pathway was substantially affected. The SCIMP deficiency led to premature termination of Erk signaling pathway activity, as judged from the reduced phosphorylation of Erk1/2, its activator, MEK1/2, and its downstream target, p90RSK, clearly demonstrating the nonredundant role of SCIMP in this process. Importantly, we were able to rescue this phenotype by reconstituting these cells with wild-type SCIMP or SCIMP with a mutated Csk binding site but not with SCIMP unable to bind SLP65. This complemented our data from CD25-SCIMP chimeras and provided a strong evidence that the main function of SCIMP is to anchor SLP65/SLP76 adaptors to the membrane, while binding of Csk drives a negative feedback loop (Fig. 8). We still do not know the precise downstream effects of SCIMP-mediated signaling on APC function. One possibility is the regulation of MHC-II induced apoptosis that is largely dependent on Erk1/2 (26). However, we did not observe any changes in the rate of apoptosis in SCIMP-depleted cells (not shown). Another possibility might be the regulation of antigen presentation. We believe that further study using SCIMP-deficient mice (currently in preparation) would shed more light on the physiological effects of signaling mediated by SCIMP.

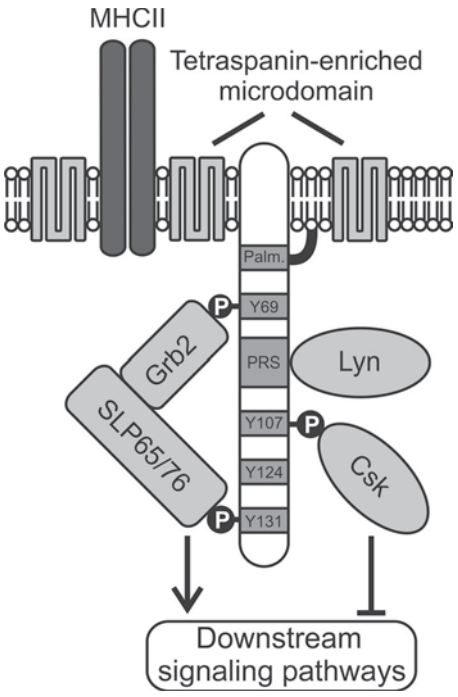

FIG. 8. A model of SCIMP-mediated signal transduction. SCIMP is palmitoylated on its submembrane palmitoylation motif (Palm.) and is localized in tetraspanin-enriched microdomains together with MHC-II. Via its proline-rich sequence (PRS), SCIMP constitutively binds the SH3 domain of Lyn kinase. Upon cross-linking of SCIMP in the immunological synapse, SCIMP becomes phosphorylated (P) at several tyrosine residues and recruits a complex of Grb2 and SLP65 or SLP76 adaptors to the plasma membrane. Subsequently, SLP65 or SLP76 initiates a signaling cascade leading to activation of downstream signaling pathways. This process is controlled by the negative regulatory kinase Csk, which is also recruited to phosphorylated SCIMP.

At present, SCIMP is the only protein in TEMs with a functional similarity to LAT, a lipid raft-associated transmembrane adaptor critically involved in signaling mediated by TCRs and other immunoreceptors. LAT interacts with the SLP family adaptor SLP76 and transduces signals of similar types to those transduced by SCIMP (16). However, the range of receptors employing SCIMP as a signal transducer will most likely be different due to its association with TEMs. We have demonstrated the importance of SCIMP in signaling via MHC-II molecules. On the other hand, many different proteins are associated with the tetraspanin web, and thus it is reasonable to speculate that more receptors dependent on SCIMP signaling will be discovered during our future efforts to understand this interesting protein.

ACKNOWLEDGMENTS

We thank all the colleagues who provided us with the cells, plasmids, and antibodies, as indicated above, and Tamiko Katsumoto for critical reading of the manuscript.

This work was supported in part by project no. AV0Z50520514, awarded by the Academy of Sciences of the Czech Republic, GACR (project MEM/09/E011), and by the Center of Molecular and Cellular Immunology (project 1M0506, Ministry of Education, Youth and Sports of the Czech Republic). P.D., O.S., and M.H. are Ph.D. stu-

dents supported in part by the Faculty of Science, Charles University, Prague, Czech Republic.

REFERENCES

1. **Al-Daccak, R., N. Mooney, and D. Charron.** 2004. MHC class II signaling in antigen-presenting cells. Curr. Opin. Immunol. **16:**108–113.
2. **Anderson, H. A., E. M. Hiltbold, and P. A. Roche.** 2000. Concentration of MHC class II molecules in lipid rafts facilitates antigen presentation. Nat. Immunol. **1:**156–162.
3. **Angelisova, P., I. Hilgert, and V. Horejsi.** 1994. Association of four antigens of the tetraspans family (CD37, CD53, TAPA-1, and R2/C33) with MHC class II glycoproteins. Immunogenetics **39:**249–256.
4. **Berditchevski, F., et al.** 2001. Analysis of the CD151-alpha3beta1 integrin and CD151-tetraspanin interactions by mutagenesis. J. Biol. Chem. **276:** 41165–41174.
5. **Bobbitt, K. R., and L. B. Justement.** 2000. Regulation of MHC class II signal transduction by the B cell coreceptors CD19 and CD22. J. Immunol. **165:** 5588–5596.
6. **Brdicka, T., et al.** 2000. Phosphoprotein associated with glycosphingolipid-enriched microdomains (PAG), a novel ubiquitously expressed transmembrane adaptor protein, binds the protein tyrosine kinase csk and is involved in regulation of T cell activation. J. Exp. Med. **191:**1591–1604.
7. **Brdickova, N., et al.** 2003. LIME: a new membrane raft-associated adaptor protein involved in CD4 and CD8 coreceptor signaling. J. Exp. Med. **198:** 1453–1462.
8. **Brown, D. A.** 2006. Lipid rafts, detergent-resistant membranes, and raft targeting signals. Physiology (Bethesda) **21:**430–439.
9. **Brown, K., D. Levitt, M. Shannon, and B. Link.** 2001. Phase II trial of Remitogen (humanized 1D10) monoclonal antibody targeting class II in patients with relapsed low-grade or follicular lymphoma. Clin. Lymphoma **2:**188–190.
10. **Cole, P. A., K. Shen, Y. Qiao, and D. Wang.** 2003. Protein tyrosine kinases Src and Csk: a tail's tale. Curr. Opin. Chem. Biol. **7:**580–585.
11. **Crotty, S.** 2011. Follicular helper CD4 T cells (TFH). Annu. Rev. Immunol. **29:**621–663.
12. **de Castro, E., et al.** 2006. ScanProsite: detection of PROSITE signature matches and ProRule-associated functional and structural residues in proteins. Nucleic Acids Res. **34:**W362–W365.
13. **Engels, N., B. Wollscheid, and J. Wienands.** 2001. Association of SLP-65/BLNK with the B cell antigen receptor through a non-ITAM tyrosine of Ig-[alpha]. Eur. J. Immunol. **31:**2126–2134.
14. **Fooksman, D. R., et al.** 2010. Functional anatomy of T cell activation and synapse formation. Annu. Rev. Immunol. **28:**79–105.
15. **Fu, C., C. W. Turck, T. Kurosaki, and A. C. Chan.** 1998. BLNK: a central linker protein in B cell activation. Immunity **9:**93–103.
16. **Fuller, D. M., and W. Zhang.** 2009. Regulation of lymphocyte development and activation by the LAT family of adapter proteins. Immunol. Rev. **232:** 72–83.
17. **Geng, L., M. Raab, and C. E. Rudd.** 1999. Cutting edge: SLP-76 cooperativity with FYB/FYN-T in the up-regulation of TCR-driven IL-2 transcription requires SLP-76 binding to FYB at Tyr595 and Tyr651. J. Immunol. **163:** 5753–5757.
18. **Grabbe, A., and J. Wienands.** 2006. Human SLP-65 isoforms contribute differently to activation and apoptosis of B lymphocytes. Blood **108:**3761–3768.
19. **Gram, H., R. Schmitz, J. F. Zuber, and G. Baumann.** 1997. Identification of phosphopeptide ligands for the Src-homology 2 (SH2) domain of Grb2 by phage display. Eur. J. Biochem. **246:**633–637.
20. **Haylett, R. S., N. Koch, and L. Rink.** 2009. MHC class II molecules activate NFAT and the ERK group of MAPK through distinct signaling pathways in B cells. Eur. J. Immunol. **39:**1947–1955.
21. **Horejsi, V., P. Otahal, and T. Brdicka.** 2010. LAT—an important raft-associated transmembrane adaptor protein. FEBS J. **277:**4383–4397.
22. **Hur, E. M., et al.** 2003. LIME, a novel transmembrane adaptor protein, associates with p56lck and mediates T cell activation. J. Exp. Med. **198:**1463–1473.
23. **Charrin, S., et al.** 2009. Lateral organization of membrane proteins: tetraspanins spin their web. Biochem. J. **420:**133–154.
24. **Jackman, J. K., et al.** 1995. Molecular cloning of SLP-76, a 76-kDa tyrosine phosphoprotein associated with Grb2 in T cells. J. Biol. Chem. **270:**7029–7032.
25. **Janssen, E., M. Zhu, W. Zhang, and S. Koonpaew.** 2003. LAB: a new membrane-associated adaptor molecule in B cell activation. Nat. Immunol. **4:**117–123.
26. **Jin, L., et al.** 2008. MPYS, a novel membrane tetraspanner, is associated with major histocompatibility complex class II and mediates transduction of apoptotic signals. Mol. Cell. Biol. **28:**5014–5026.
27. **Kawabuchi, M., et al.** 2000. Transmembrane phosphoprotein Cbp regulates the activities of Src-family tyrosine kinases. Nature **404:**999–1003.
28. **Koretzky, G. A., F. Abtahian, and M. A. Silverman.** 2006. SLP76 and SLP65: complex regulation of signalling in lymphocytes and beyond. Nat. Rev. Immunol. **6:**67–78.
29. **Krogh, A., B. Larsson, G. von Heijne, and E. L. L. Sonnhammer.** 2001. Predicting transmembrane protein topology with a hidden Markov model: application to complete genomes. J. Mol. Biol. **305:**567–580.
30. **Kropshofer, H., et al.** 2002. Tetraspan microdomains distinct from lipid rafts enrich select peptide-MHC class II complexes. Nat. Immunol. **3:**61–68.
31. **Lang, P., et al.** 2001. TCR-induced transmembrane signaling by peptide/MHC class II via associated Ig-alpha/beta dimers. Science **291:**1537–1540.
32. **Li, S. S.** 2005. Specificity and versatility of SH3 and other proline-recognition domains: structural basis and implications for cellular signal transduction. Biochem. J. **390:**641–653.
33. **Lingwood, D., H. J. Kaiser, I. Levental, and K. Simons.** 2009. Lipid rafts as functional heterogeneity in cell membranes. Biochem. Soc. Trans. **37:**955–960.
34. **Mittelbrunn, M., M. Yanez-Mo, D. Sancho, A. Ursa, and F. Sanchez-Madrid.** 2002. Cutting edge: dynamic redistribution of tetraspanin CD81 at the central zone of the immune synapse in both T lymphocytes and APC. J. Immunol. **169:**6691–6695.
35. **Muller, K., et al.** 1996. Rapid identification of phosphopeptide ligands for SH2 domains. Screening of peptide libraries by fluorescence-activated bead sorting. J. Biol. Chem. **271:**16500–16505.
36. **Nadolski, M. J., and M. E. Linder.** 2007. Protein lipidation. FEBS J. **274:** 5202–5210.
37. **Nagy, Z. A., et al.** 2002. Fully human, HLA-DR-specific monoclonal antibodies efficiently induce programmed death of malignant lymphoid cells. Nat. Med. **8:**801–807.
38. **Patterson, H. C., M. Kraus, Y. M. Kim, H. Ploegh, and K. Rajewsky.** 2006. The B cell receptor promotes B cell activation and proliferation through a non-ITAM tyrosine in the Igalpha cytoplasmic domain. Immunity **25:**55–65.
39. **Resh, M. D.** 2006. Palmitoylation of ligands, receptors, and intracellular signaling molecules. Sci. STKE **2006:**re14.
40. **Riol-Blanco, L., et al.** 2009. Immunological synapse formation inhibits, via NF-[kappa]B and FOXO1, the apoptosis of dendritic cells. Nat. Immunol. **10:**753–760.
41. **Rodriguez-Pinto, D.** 2005. B cells as antigen presenting cells. Cell Immunol. **238:**67–75.
42. **Rubinstein, E., et al.** 1996. CD9, CD63, CD81, and CD82 are components of a surface tetraspan network connected to HLA-DR and VLA integrins. Eur. J. Immunol. **26:**2657–2665.
43. **Sala-Valdes, M., et al.** 2006. EWI-2 and EWI-F link the tetraspanin web to the actin cytoskeleton through their direct association with ezrin-radixin-moesin proteins. J. Biol. Chem. **281:**19665–19675.
44. **Sauer, K., et al.** 2001. Hematopoietic progenitor kinase 1 associates physically and functionally with the adaptor proteins B cell linker protein and SLP-76 in lymphocytes. J. Biol. Chem. **276:**45207–45216.
45. **Savina, A., and S. Amigorena.** 2007. Phagocytosis and antigen presentation in dendritic cells. Immunol. Rev. **219:**143–156.
46. **Sonnhammer, E. L., G. von Heijne, and A. Krogh.** 1998. A hidden Markov model for predicting transmembrane helices in protein sequences. Proc. Int. Conf. Intell. Syst. Mol. Biol. **6:**175–182.
47. **Unternaehrer, J. J., A. Chow, M. Pypaert, K. Inaba, and I. Mellman.** 2007. The tetraspanin CD9 mediates lateral association of MHC class II molecules on the dendritic cell surface. Proc. Natl. Acad. Sci. U. S. A. **104:**234–239.
48. **Wan, J., A. F. Roth, A. O. Bailey, and N. G. Davis.** 2007. Palmitoylated proteins: purification and identification. Nat. Protoc. **2:**1573–1584.
49. **Yanez-Mo, M., O. Barreiro, M. Gordon-Alonso, M. Sala-Valdes, and F. Sanchez-Madrid.** 2009. Tetraspanin-enriched microdomains: a functional unit in cell plasma membranes. Trends Cell Biol. **19:**434–446.